

An Experimental Study for the Behavior of Slender Steel Built Up Girders

Ehab B. Matar

A Structural Engineering Dept., Faculty of Engineering, Zagazig University, Zagazig- Egypt
Ehab_bmatar@yahoo.com

Abstract: Slender steel sections are nowadays widely used for the wide spread production of higher strength steel material which results in a reduced steel weight, high technological welding procedures and the availability of powerful computer software that can deals with different plates buckling modes. Slender steel beams needs special attention regarding the probability of occurrence of local buckling in web or flanges or the occurrence of shear buckling in web before achieving the yielding moment or the plastic moment capacity. However, the difference in identifying the limits of width / thickness ratio for different components of beams classes in different codes highlight a question about the creditability and conservative assumptions in different codes. In this paper; a comparison between failure load from experimental work and the predictions driven by the AISC, and the ECP is carried out.

[Ehab B. Matar. **An Experimental Study for the Behavior of Slender Steel Built Up Girders.** *Life Sci J* 2013;10(2):2281-2289] (ISSN:1097-8135). <http://www.lifesciencesite.com>. 319

Key word: slender, steel, local, buckling, beams

1. Introduction

High strength steel is now widely used for longer bridge spans, taller buildings,...etc. The driving force for using high strength steel is in the first place economy; but there is also an environmental interest in saving resources. A peer review for the plate buckling, local buckling and post buckling strength of steel plates were presented by Galambos (1998). The effective width concept developed by Winter, Von Kármán ...etc. and their developed equations for calculating the effective widths were presented. A discussion for the interaction between plate elements and buckling modes of a plate assembly in the form of I or box sections are pointed out in three principle modes: mode I of purely local buckling mode which involves out of plane deformation of the component plates with the junctions remaining essentially straight, mode II in which the buckling process involves in plane bending of one or more of the constituent plates as well as out of plane bending of all the elements and finally mode III in which the plate structure may buckle as a column in flexural or flexural torsional buckling mode with or without interaction with local buckling.

Škaloud *et al.* (1999) reported about a series of fatigue testing of a series of plate girders (with high web slenderness =320) subjected to repeated predominantly shear and tested at Klokner Institute in Prague. It was found that if compared with the fatigue performance of less slender webs (with web slenderness =250), the initiation of fatigue cracks occurred after substantially lower number of load cycles and the fatigue cracks grew more speedily so that the fatigue failure was a considerably faster phenomenon. Kazuo, *et al.* (1999) presents experimental results of the ultimate behavior and

strength of plate girders with large aspect ratio and web width to thickness ratios under sagging moment and shear. It was concluded that composite girders with large aspect ratio of 3 and with large web width to thickness ratio up to 158 can be used effectively in bridges. André *et al.* (2002) used non-linear finite elements to study the effect of initial imperfections in numerical simulations of slenderness of plated structures. They concluded that the choice of this initial imperfection has a significant influence on the computed collapse load. Milan *et al.* (2002) presented some design rules for hybrid girders together with justification. Typically hybrid girders are of cross section class 4 according to Eurocode 3. The questions of ultimate strength and post buckling behavior of slender plate girders subjected to patch loading such as girders of steel and composite bridges have been dealt with by Kuhlmann (2002). A complementary parametric study using ANSYS commercial FE package demonstrated a high increase of the ultimate load for closed section stiffeners and long patch loads in comparison to short patch loads. Goyet *et al.* (2002) mentioned some ambiguities regarding the way the so called relative flexural rigidity calculations. They concluded that EC3 specifications can only be expected to provide conservative ultimate loads if stiffeners are fitted with an appropriate effective sheet width when characterizing their flexural rigidity. Bambach and Rasmussen (2005) reported the plastic effective width equations and inelastic design models for slender I-sections and slender channels in minor axis bending. Bambach (2006) presents experimental and numerical studies of un-stiffened plates and sections that contain them in both compression and bending, and in particular analyses the mechanism that provides post buckling strength. It is shown that un-

stiffened elements under any stress gradient have significant post local buckling strength, the mechanism for which is the redistribution of longitudinal stress in the element away from the buckled regions towards the un-buckled regions. In slender un-stiffened elements this redistribution may occur to such an extent that tensile stresses develop in axially compressed elements. Halme *et al.* (2008) reported about difficulty of using extra or ultra high strength steels in the current versions of most of the European standards and Eurocode 3 as they restricts the validity of equations for computing local buckling resistance to steel with yield strength less than 700 MPa. New experimental data generated for slender high strength steel profiles are mentioned with a development of current effective width equation for local buckling of class 4 cross section in the Eurocode 3 to be valid of steels with yield strength more than 700 MPa. Abspoel (2008) mentioned that plate girders with a slender web having a very high bending moment capacity relative to their self weight, and could be of economical interest for all kinds of structures. Hagen *et al.* (2008) presents an attempt based on extensive numerical simulations of girders with different web slenderness and openings configurations to determine shear capacity of plate girders. Schafer and Seif (2009) carried out a nonlinear finite element analysis for braced slender steel columns and beams and compared the results to three design methods AISC, AISI and DSM. They have found that AISC predictions are excellent when the section is compact while for sections with non-compact AISC was un-conservative. For slender steel sections the AISC was excessively conservative.

Sinur and Beg (2011) investigate the influence of intermediate stiffener on the behavior of longitudinally stiffened plated girders through testing two specimens (11000mm span each) using two profiles of longitudinal stiffeners. They concluded that the requirements for the transverse stiffener design according to EN 1993-1-5 have been found conservative i.e. they were designed to take into account 50% of the tension field action and it is still stronger than needed. Bedynek *et al.* (2011) investigated the shear and shear bending interaction of tapered steel plate girders. Four half scale prototypes were tested in the laboratory of Structural Technology (UPC, Spain) to study this subject and verifying numerical model. While EN 1993-1-5 was conservative in calculating the ultimate shear load for two prototype specimens I, II, it overestimates the ultimate shear load for the other two specimens III, IV and concluded that the recommended proposal included in EN 1993-1-5 for tapered plate girders cannot be treated, in some cases, as a reliable design tool. Ishac *et al.* (2012) carried out a numerical

analysis using non linear finite elements for slender plate girders. The effect of horizontal stiffeners existence in web panel and the increase of its aspect ratio were presented in this study. The parametric study indicates an effect of the existence of the horizontal stiffeners on the final failure load of the plate girders. Alinia *et al.* (2012) investigated the inelastic buckling and post buckling behavior of stocky plates under combined shear and in plane bending stresses and compared to slender plates using theoretical P-Ritz energy method and numerical nonlinear FE method. They observed that whereas in slender plates, elastic buckling occurs prior to the material's proportional limit load, stocky plates buckle in an inelastic way within the post-yield stage. In addition, it was observed that the classic interaction equation overestimates buckling loads; and therefore, a modified equation that can safely be applied to stocky and slender plates is proposed. Chica *et al.* (2013) presented some recommendations for FEM assessments of plates sections in bridges that take the initial imperfections, geometric imperfections and residual stresses for high strength slender steel plates. They concluded that regarding the considerations of initial imperfections, the recommendations of Annex C of Eurocode 3 parts 1-5 (CEN, 2006) provide good results, in general. The use of imperfections shapes based on the expected failure shape and amplitudes in the range of the fabrication tolerances is recommended. Moreover, they concluded that it is not necessary to use initial residual stress in the FEM stress patterns based on real measured residual stresses and the results obtained with the proposed simplified rectangular pattern used in this paper based on a rectangular distribution of membrane stresses are in good agreement with the test results.

2. Experimental Program Objectives

Knowledge based on static tests plays an important verification for the code design equations. The experimental program was designed to study the effect of variation of the web depth/ thickness ratio and flange width/ thickness ratio for different slender steel plate girders without longitudinal stiffeners. Behavior of the slender steel girders are captured by tracing the strains, lateral displacements of compression flange and vertical deflection for all specimens during the loading course up to failure to understand the distribution of stress prior, during and after local buckling occurrence.

Specimens' Description

Eight steel plate girders were fabricated from built up sections with dimensions as shown in Figure (1) and table (1). The nominal dimensions of different specimens as well specimen names are summarized in that table. It was tried as much as possible (depending

on available plate thickness) to maintain the cross sectional area of the steel beams nearly constant and redistribute the material between the web and flanges

and the maximum cross sectional area deviates from the average one of the eight specimens by 14.67%.

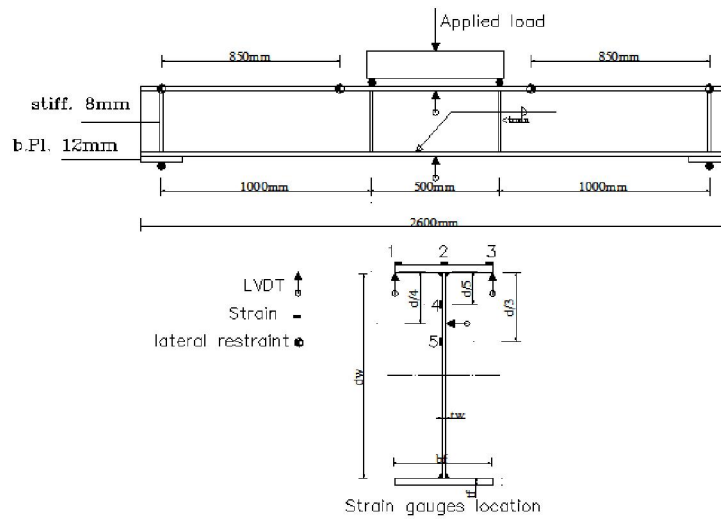


Figure (1): steel plate girders

Coupons of the steel plates were taken and upon testing it was found that the yield and ultimate tensile stresses were 417 and 566 MPa respectively while the percentage elongation was 15%. All the base plates at bearing location were of 12mm thickness. Each specimen was assigned with a unique name describing the type of section "B" for beams, the nominal flange width/thickness ratio, and then, the nominal web depth

/thickness ratio are mentioned in sequence. Therefore, B10-149 is a steel beam with flange width/thickness ratio of nearly 10 and nearly web depth/ thickness ratio of 149. As shown in that table; the flange width/thickness ratio ranged between 10 and 26 while the web depth / thickness ratio ranged between 74 and 14

Table (1) Geometrical dimensions and instrumentation for different specimens

Specimen	b_f (mm)	t_f (mm)	d_w (mm)	t_w (mm)	Cross sectional area (mm ²)	Strain gauges location	LVDT location
B10-74	130	6	300	4	2760	1,2,3,4,5	L/2,d/4,1,3
B10-124	95	4	500	4	2760	2,4,5	L/2,d/4
B10-134	95	4	540	4	2920	2,4,5	L/2,d/4
B10-149	95	4	600	4	3160	2,4,5	L/2,d/4
B12-109	110	4	440	4	2640	1,2,3,4,5	L/2,d/4,1,3
B17-99	150	4	400	4	2800	1,2,3,4	L/2,1,3
B21-99	180	4	400	4	3040	1,2,3,4	L/2,1,3
B26-99	220	4	400	4	3360	1,2,3,4	L/2,1,3

The specimen B10-149, was failed at early stage of loading course due to instability of the specimen and the loading system. A reference specimen B10-74 of non-compact section; according to the Egyptian Code of Practice (ECP), was chosen for comparison with other slender steel sections. It is worth noting that the ECP classifies any section composing either of slender web and/or slender flange as a slender section.

Tests were carried out at structural laboratories of the Faculty of Engineering, Zagazig University, Egypt.

Instrumentation and Test Setup

Locations of strain gauges and LVDT for different specimens as well photos for a sample of instrumentation are shown in Figure (2).



Figure (2): Photos for the instrumentation of some specimens

All the tested beams are subjected to four points bending loaded by a frame testing machine of maximum capacity of 250 KN and the load is applied through a hydraulic jack applied over a load cell on specimen. Strain gauges are positioned at mid span of all specimens. The LVDT's were also used to measure the local buckling deformation at flanges' tip and at different locations through depth of web. A data logger was used to capture load values, strains and LVDT readings during the load course. All specimens were restrained against lateral torsional buckling by using special steel guides of stiffened U frames at supports

and at one third span points so that they can restrain lateral movement of compression flange only and do not result in any restraints to the vertical movement of the specimen.

3. Discussion of Experimental Results Load Deflection Relationship for Different Specimens

The load deflection relationship was captured by measurement of the vertical displacement of lower flange plate using displacement transducers (LVDT).

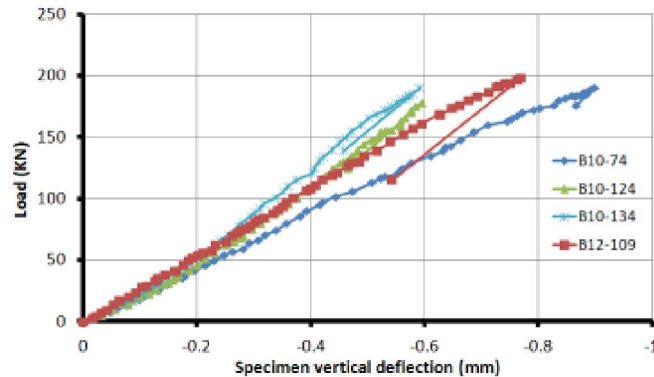


Figure (3): Load- deflection relationship for slender web specimens

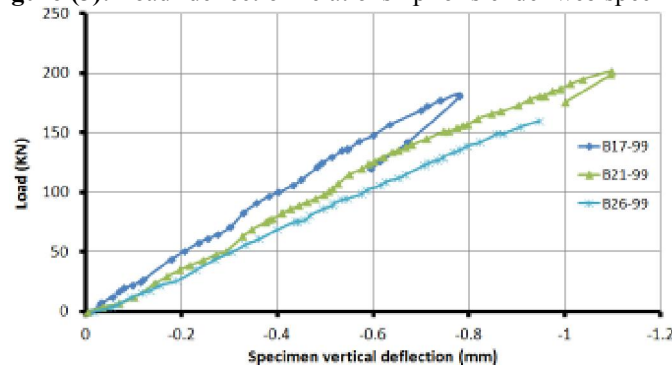


Figure (4): Load-deflection relationship for slender flange specimens

The deflection is shown in Figures (3) and (4) for specimens with slender web and others with slender

flanges respectively. As shown for slender web specimens shown in Fig. (3), in comparison with the

reference specimen B10-74, the deflection was lower for slender web specimens due to the use of larger depths and lower thickness of web plates. For example, specimen B10-134 recorded at failure load (which is similar to B10-74) a deflection value of nearly two thirds of that deflection recorded for specimen B10-74. On the other hand, the larger the flange slenderness the higher the deflection values recorded. This may be attributed to the occurrence of local buckling for higher flange slenderness which will

affect the overall stiffness of the beam and will increase accordingly the recorded deflection as shown in Fig. (4).

Flange local buckling deformation for slender flange specimens

The relationship between the vertical load and the compression flange tips deformation are recorded for specimens with varying flange slenderness as illustrated in Figure (5).

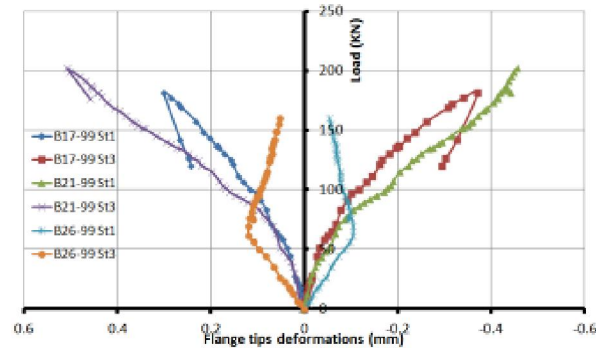


Figure (5): Load-flange tips deformation relationship for slender flange specimens

As shown in that figure; that, the recorded vertical deformations at the flange tip (stations 1 and 3) are reversible in sign for each specimen. This

indicates the formation of a flange local buckling wave on each side of the web as clarified by photos in Figure (6).



Figure (6): local buckling for slender flange specimens during loading course and after failure

The larger the flange slenderness; the larger the deformations recorded for different specimens. However, as shown in Figure (5) that specimen B26-99 recorded largest deformation till 63KN and then, the deformation reduced due to the mechanism for which is the redistribution of longitudinal stress in the element away from the buckled regions towards the un-buckled regions. In slender un-stiffened elements this redistribution may occur to such an extent that tensile stresses develop in axially compressed elements as confirmed by Bambach (2006).

Web local buckling deformation for slender web specimens

The relationship between the vertical load and the web local buckling deformation measured at one fourth the web height is clarified for two slender web specimens as shown in Fig. (7). In that sample figure, it is clarified that the larger the web slenderness the larger the web local buckling deformation. For example, the deformation at 80KN was nearly 50% greater for B10-134 compared to that recorded for B12-109. This increase was much less at the end course of the loading at failure where the difference was nearly 25% greater for B10-134.

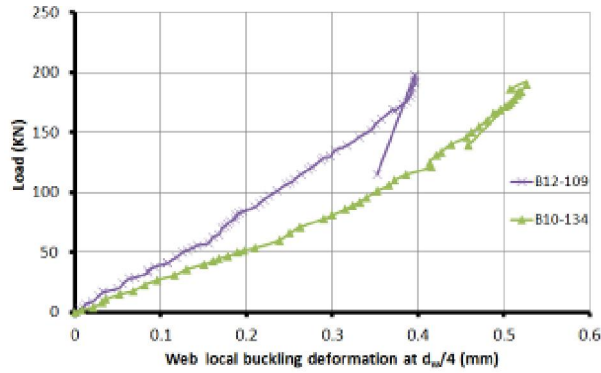


Figure (7): local buckling for slender web specimens during loading course

Load –web strain relationship for slender web specimens

The relationship between the vertical load and the average strain recorded for specimens with varying web slenderness is illustrated in Figure (7). The load strain relationship indicates higher strain measurements for slender web specimen B10-134

compared to the lower slenderness web B10-74. For example the strain for the web at failure load (which is almost the same for both specimens) for B10-134 recorded an increase of nearly 50% compared with B10-74. This may be attributed to the greater contribution of the web to the flexural stiffness of B10-134 (nearly 48.3%) than for B10-74 (nearly 20%).

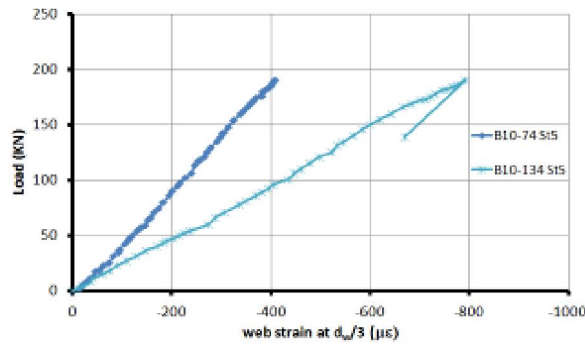


Figure (8): Load-strain relationship for slender web specimens

On the other side, a plateau for the strain distribution along the compression portion of the depth of the web i.e. at channels 2, 4 and 5 is shown in Figure (9). As shown in that figure the strain

distribution was linear at the beginning of the loading course then deviate from linearity starting nearly from 39% of the failure load and at later stages due to web local buckling.

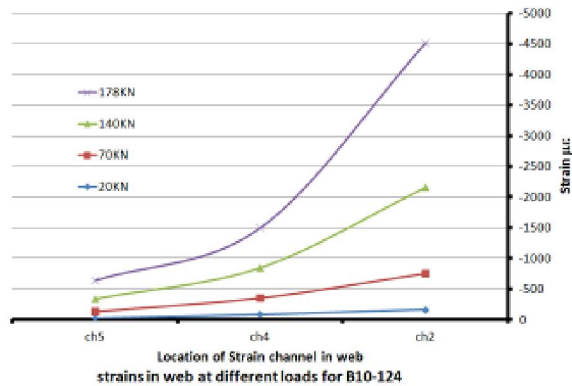


Figure (9): plateau of the strain distribution in the compression portion of the web

Load –flange strain relationship for slender flange specimens

The strain distribution across the flange stations for two specimens B26-99 and B10-74 is shown in Figure (10). As shown in that figure that, for specimen B26-99; the compression flange resists the compressive bending stresses till nearly 60KN (nearly 38% of the failure load) and then local buckling starts at one flange tip (station 1). Then, a redistribution of the forces occurred for the compressive bending stresses followed by remarkable increase in strain at station 2 and 3 and a decrease for station 1 till reach tension while the other flange tip starts to local

buckled similarly to station 1. As confirmed by Bambach (2006); that in slender un-stiffened elements redistribution of stresses following local buckling may occur to such an extent that tensile stresses develop in axially compressed elements. For B10-74, we have nearly linear strain distribution across the flange stations till nearly 63% of the failure load when the flange tips reached the yield strain then the strain distribution becomes non-linear. The flanges with lower slenderness can reach the yield strain prior to occurrence of local buckling while those with slender flanges can not usually attain the yield strain prior to local buckling.

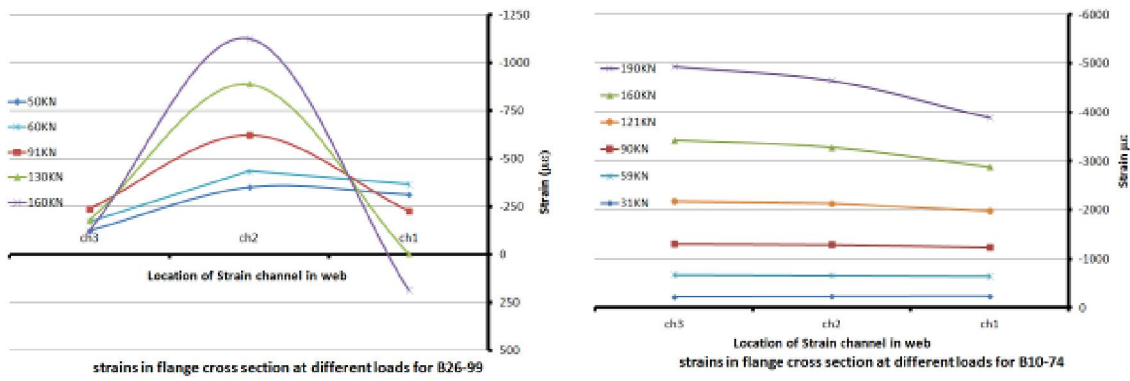


Figure (10): Load-Flange strain distribution for different flange slenderness specimen

Comparison of failure loads for different tested specimens

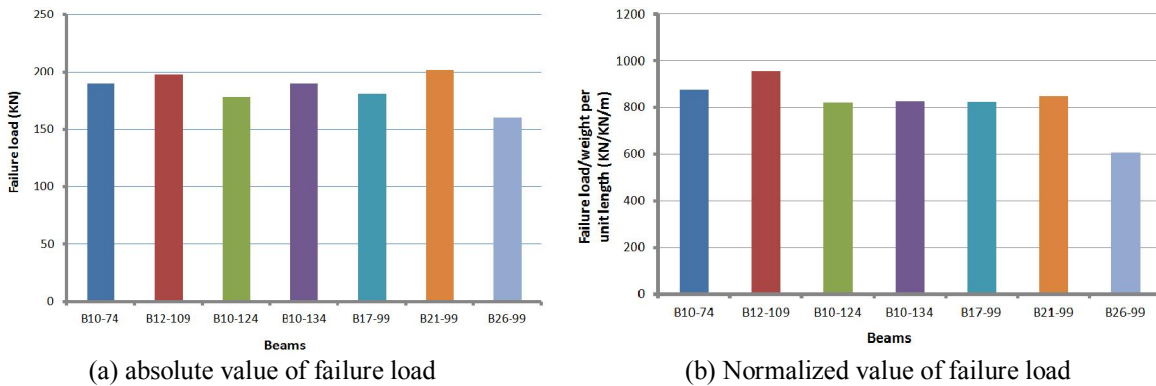


Figure (11): failure load for all specimens

Figure (11) shows a comparison of the failure loads for different specimens. Originally, all the beams were designed to discard shear buckling failure and to fail with local buckling and this is what was achieved. However, most specimens' cross sectional area vary compared to average nominal cross section by nearly -9% to +15%. Except the specimen B26-99 with the highest value of the slenderness ratio of flange, most

failure loads were relatively close for different specimens as shown in Fig.11(a). The failure load ranged between 160KN (for specimen B26-99) and 202 KN (for specimen B21-99) with a maximum variation compared to the average failure load between +8.9% and -13.78%. Comparison of the absolute value of failure load may be deceiving as it does not indicate the change of cross sectional area (and therefore

flexural rigidity) in different specimens. Therefore, as a trial to better understanding the results, a normalization of the failure load was carried out by dividing its value with the weight per unit length for the beam and then comparing as shown in Fig. 11 (b). In that figure, it is clarified that specimen B12-109 (with relatively slender web and close flange slenderness to non-compact class according to ECP) yields the maximum failure load and the lowest weight. This specimen recorded an absolute failure load of 198KN i.e. 98% of the maximum value recorded for B21-99.

Comparison of Failure Loads with theoretical Values Predicted in Different Codes for All Specimens

Comparison between the failure load resulted from experimental work and that predicted by both of the AISC and ECP using LRFD method of design for

both codes, indicates the need to further continue work and development the enhancement and adjustment of the design equations for both codes. While the failure loads predicted by the ECP-LRFD were over-conservative for all for slender flange sections specimens (B17-99, B21-99, B26-99) it was un-conservative for slender web sections and non compact sections (B10-134, B10-124 and B10-74 respectively). The failure loads predicted by the AISC-LRFD for slender built up section were un-conservative for slender web specimens and over-conservative for slender flange specimens. This observation regarding AISC was also mentioned by Schafer and Seif (2009) and a further adjustment is needed to overcome this observation by further development of design code equations depending on experimental testing of closer full scale specimens and finite elements studies.

Table (2) Comparison between experimental failure load and that predicted by AISC and ECP

specimen symbol	A_{gross} (mm ²)	Experimental Failure load (KN)	ECP-LRFD		AISC-LRFD	
			P_{theo} (KN)	P_{exp}/P_{theo}	P_{theo} (KN)	P_{exp}/P_{theo}
B10-74	2760	190	234.08	0.81	221.97	0.86
B12-109	2640	198	164.89	1.20	205.35	0.96
B10-124	2760	178	217.12	0.82	247.16	0.72
B10-134	2920	190	238.79	0.80	269.18	0.71
B17-99	2800	181	93.28	1.94	141.15	1.28
B21-99	3040	202	73.14	2.76	111.67	1.81
B26-99	3360	160	56.47	2.83	86.94	1.84

Conclusion

An experimental program was executed to investigate the behavior of slender steel beams. Seven specimens representing slender built up girders of span length of 2500mm were tested under four point bending. The slenderness of the flanges was varied between 10 and 26 while the slenderness of the webs was varied between 74 and 134. Specimens failed with local buckling either in flange and/or web in pure moment region with no sign of shear buckling. Both of the AISC and ECP needs further adjustments for the design equations related to slender sections depending on further both experimental and numerical finite elements studies.

References

1. Theodore V. Galambos; "Guide to stability design criteria for metal structures"; John Wiley & sons Inc.; 5th edition, 1998
2. Miroslav Škaloud, Petr Broz, Martin Novák, "Experimental and theoretical investigation into the breathing of thin-walled steel girders"; 2nd European conference on steel structures, May 26-29, 1999, Praha, Czech Republic.
3. Kazuo Ohgaki, Jun-ichi Yabe and Yoshi Fumi Kawaguchi; "Experimental study on ultimate strength of plate girders with large web aspect ratio and web width to thickness ratio"; 2nd European conference on steel structures, May 26-29, 1999, Praha, Czech Republic.
4. André , H.Degée, V. de Ville de Goyet and R. Maquoi; "Effect of initial imperfections in numerical simulations of collapse behavior of stiffened plates under compression"; Proceedings of the third European conference on steel structures, 19-20 sept. 2002, Coimbra, Portugal.
5. Milan Veljkovic and Bernt Johansson; "Design of hybrid steel girders"; Proceedings of the third

- European conference on steel structures, 19-20 sept. 2002, Coimbra, Portugal.
6. Ulrike Kuhlmann and Martin Seitz; "Behavior of longitudinally stiffened girder webs subjected to patch loading"; Proceedings of the third European conference on steel structures, 19-20 sept. 2002, Coimbra, Portugal.
 7. V. de Ville de Goyet, R. Maquoi, Fr. Bachy and I. André; "Ultimate load of stiffened compressed plates: effects of some parameters and discussion concerning the EC3 Rules"; Proceedings of the third European conference on steel structures, 19-20 sept. 2002, Coimbra, Portugal.
 8. Michael R Bambach, Kim JR Rasmussen, (2005) "Elastic and Plastic effective width equations for un-stiffened elements under stress gradient"; Proceedings of the fourth European conference on steel and composite structures, 8-10 June. 2005, Maastricht, The Netherlands.
 9. M.R. Bambach, (2006); "Local buckling and post local buckling redistribution of stress in slender plates and sections"; Journal of Thin Walled Structures 44 (2006), pp 1118-1128.
 10. Tapani Halme, Lauri Huusko, Gary Marquis and Timo Björk; "Local buckling of plates made of high strength steel"; Proceedings of the 5th European conference on steel and composite structures, 3-5 Sept. 2008; Graz, Austria.
 11. Roland Abspoel; "The maximum web slenderness of plate girders: State of the art and Laboratory tests"; Proceedings of the 5th European conference on steel and composite structures, 3-5 Sept. 2008; Graz, Austria.
 12. N. C. Hagen and P. K. Larsen; "Design of slender girders with large rectangular web openings"; Proceedings of the 5th European conference on steel and composite structures, 3-5 Sept. 2008; Graz, Austria.
 13. B. W. Schafer and Seif, M., "Finite element comparison of design methods for locally slender steel beams and columns" In Proceedings of the structural stability research council's annual stability conference, pp. 69-90. (2009)
 14. Franc Sinur and Darko Beg; "Numerical and Experimental Analysis of Intermediate transverse stiffener in Stiffened Plated girder"; Proceedings of the 6th European conference on steel and composite structures, Aug. 31- Sept. 2nd, 2011; Budapest, Hungary
 15. Agnieszka Bedynek, Esther Real and Enrique Mirambell; "Tapered steel plate girders Experimental and numerical investigation on shear and shear-bending interaction"; Proceedings of the 6th European conference on steel and composite structures, Aug. 31- Sept. 2nd, 2011; Budapest, Hungary
 16. Ishac ISHAC, Ossama EL HOSSEINY, Ehab MATAR and Shady MANDOUR; "Behavior Analysis of Stiffened Slender Plate Girders"; Proceedings of the Global Thinking in Structural Engineering: Recent Achievements IABSE Conference, May 7-9, 2012; Sharm El Sheikh, Egypt.
 17. M.M. Alinia, Ghazaleh Soltanieh, Mozhdeh Amani; "Inelastic buckling behavior of stocky plates under interactive shear and in-plane bending"; Thin-walled Structure 55(2012), pp 76-84.
 18. J.A. Chica, J.T. San Jose, F. Millanes, J.M. Manso; "Recommendations on imperfections in the design of plated structural elements of bridges" Journal of Constructional Steel Research 86 (2013), pp 183-194.
 19. "Specification for Structural Steel Buildings" AISC-LRFD, June, 2010.
 20. "Egyptian Code of Practice for Steel Construction and Bridges (Load and Resistance Factor Design)" Code No. ECP 359-2007, edition 2008.

6/5/2013